Journal of Thermodynamics & Catalysis - Open Access

Research Article
OPEN ACCESS Freely available online
doi:10.4172/2157-7544.1000101

Synthesis of HMOR and HZSM-5 and their Behaviour in the Catalytic Conversion of Methanol to Propylene (MTP)

Juan Carlos Moreno-Piraján[1]*, Vanessa S. Garcia-Cuello[1] and Liliana Giraldo[2]

[1]*Facultad de Ciencias, Departamento de Química, Grupo de Investigación en Sólidos Porosos y Calorimetría, Universidad de los Andes, Bogotá, Colombia, USA*
[2]*Facultad de Ciencias, Departamento de Química, Universidad Nacional de Colombia, USA*

Abstract

The zeolites HZSM5 and HMOR were synthesized and their behavior analyzed during the conversion from methanol to propylene (MTP). These zeolites were studied with XRD, SEM, NH_3-TPD, nitrogen adsorption at 77 K and adsorption microcalorimetry. It was established that acidity influences the conversion of methanol to propylene. The development of mesopores in HMOR allowed the process to be more selective for MTP process. The role that acid and basic sites and the ratio Si/Al play in the conversion process was determined.

Keywords: Adsorption microcalorimetry; Conversion methanol; HMOR; HZSM5; MTP

Introduction

Mordenite is a zeolite that has an orthorhombic structure with the dimensions of a unit cell [1-5] of: a ¼ 18:13) b ¼ 29:49) c ¼ 7:52). As mordenite has a Si/Al molar ratio ≥5, it is very resistant to severe thermal and chemical treatments. At a Si/Al molar ratio equal to 5 the completely hydrated sodium form has the ideal composition of $Na_8Al_8Si_{40}O_{96}.24H_2O$ [1-10]. The mordenite structure consists of two channel systems: an elliptical pore channel (12MR 6.7×7.0 Å), which runs parallel to the c-axis, and another channel that runs parallel to the b-axis (8MR 2.6×5.7 Å). Due to its high thermal and acid stability, mordenite has been used as a catalyst for important reactions, such as hydrocracking, hydroisomerization, alkylation, reforming, dewaxing and the production of dimethylamines [11-24]. Mordenite has also been used in the adsorptive separation of gas or liquid mixtures [25-30]. In addition, mordenite has been considered for use in semiconductors, chemical sensors and nonlinear optics [30-34].

The HZSM-5 zeolite is active in several reactions such as alkylation, isomerization, disproportionation and cracking. Acidity is one of the most important characteristics of zeolites that make them catalytically important. HZSM-5 contains both Lewis and Bronsted acid sites. In order to accurately evaluate the catalyst and the product selectivity pattern, it is essential to estimate not only the total acidity but also to quantify the number of Bronsted and Lewis sites and their strength. The relative acidity of the reactant molecule as well as the quantitative distribution of the type of different acid sites will determine the catalytic activity. There are many reports on the relationship between the acidity of zeolites and their catalytic activity [1-19, 35-40]. Various methods such as titration, gravimetric adsorption, temperature programmed desorption of bases, calorimetric measurement and the infrared spectroscopy of adsorbed species have been used to measure the acidity of zeolites [1-17]. In the modern petrochemical industry, propylene serves as an essential feedstock for the production of various polypropylene plastics, acrylonitrile, propylene oxide and many other commodity chemicals that can be used as substitutes for non-plastic materials such as paper, steel and wood. So far its market demand has been increasing steadily. Propylene, however, has always been produced as the byproduct of steam cracking and catalytic cracking of crude oil. Without exception such routes rely on the catalytic transformation of petroleum. Because of the petroleum crisis, finding a new way to produce propylene has attracted much interest. Numerous studies have examined the promoters of the catalysts for the MTO reaction, and have found that impregnation with lanthanum and silver can improve the C_2–C_4 alkene selectivity from 38.9% to 56.0% because of a reduction in the apparent pore size of the zeolite channels [43-49]. Previous work [50-64] revealed that phosphorus modification led to a significant decrease in activity and increased the yield of light alkenes from methanol. It has been reported that entrained phosphate is an impediment to the sterically demanding reactions of methanol conversion [65-70]. Other studies [71-72] investigated the deactivation and product distribution of the MTO process over a phosphorus-modified HZSM-5 catalyst, on which propylene selectivity reached about 40%. However, there are few reports concerning the MTP process [22-32]. Little research exists on the effect of phosphorus on the selective conversion of methanol to a specific olefin, in particular, propylene. This work shows the catalytic effects of HMOR and HZSM-5 in the conversion of methanol to propylene, and their selectivity, and the results are compared with those reported in the literature.

Experimental

Mordenite synthesis by standard procedure

A gel with the composition $6Na_2O:Al_2O_3:30.SiO_2:780.\ H_2O$ was prepared. First, 4.75g NaOH were dissolved in 10g water. To this solution 3.575g of sodium aluminate were added, and the mixture was stirred (350 rpm) until dissolution. Thereafter, 161.25g of H_2O were added. Finally, 24.55g of SiO_2 were added; the mixture was stirred (350 rpm) for 30 min. The gel was transferred to Teflon-lined stainless steel autoclaves (60 mL capacity). The crystallization temperature was 170°C. The influence of crystallization time (12, 24 and 36 h) and seed addition was studied. A commercial mordenite (Zeolyts, SiO_2/Al_2O_3=35) acquired from Conshohocken, PA 19428-2240, USA was used as the seed (5 mg of seed for 204,125g of gel).

***Corresponding author:** Juan Carlos Moreno-Piraján, Facultad de Ciencias, Departamento de Química, Grupo de Investigación en Sólidos Porosos y Calorimetría, Universidad de los Andes, Bogotá, Colombia, USA, Tel: (571) 3394949, E-mail: jumoreno@uniandes.edu.co

Received August 17, 2010; **Accepted** October 14, 2010; **Published** October 16, 2010

Citation: Moreno-Piraján JC, Garcia-Cuello VS, Giraldo L (2010) Synthesis of HMOR and HZSM-5 and their Behaviour in the Catalytic Conversion of Methanol to Propylene (MTP). J Thermodyn Catal 1:101. doi:10.4172/2157-7544.1000101

HZSM5 synthesis by hydrothermal method

Synthesis of zeolite ZSM-5: ZSM-5 zeolite was synthesized by simultaneously adding appropriate amounts of an alkaline sodium aluminate solution and an acid solution to the solution of Ludox under agitation. The first solution was prepared by dissolving sodium aluminate with sodium hydroxide in distilled water and the second one by dissolving sulphuric acid and tetrapropylammonium bromide in distilled water. The mixture obtained had the following molar composition: 0.012 Al_2O_3, 0.27 Na_2O, 0.1 TPABr, 0.2 H_2SO_4, 1 SiO_2 and 54 H_2O [23]. The gel formed was stirred vigorously at room temperature for 2 h, and put in a PTFE-lined stainless steel autoclave and treated at 150°C for 24 h under autogenous pressure, as shown in Figure 1. After synthesis, the product was filtered, washed with deionized water and dried at 80°C for 12 h. In order to prepare the exchanged forms of ZSM-5 zeolite, the synthesized material was heated to 550°C for 5 h under atmospheric conditions.

Preparation of H-ZSM-5 zeolite: The H-form of ZSM-5 zeolite was prepared as follows the procedure reported in literature [11]: ZSM-5 zeolite was stirred in a 1 mol L^{-1} aqueous ammonium chloride solution for 24 h at room temperature. The NH_4-ZSM-5 obtained was recovered by filtration, washed with distilled water and dried at 80°C for 12 h. After that, the solid was converted to the H-form at high temperature (550°C) for 12 h under atmospheric conditions.

Methods of characterization

The powder XRD patterns were obtained with CuKa 1 radiation (k = 1.5406 Å) on a RIGAKU Miniflex model benchtop diffractometer. Thermal analysis (TGA, DTA) was performed in air using a NETZSCH STA 409PC DTA–TGA analyser. All samples were heated to 1000°C at a heating rate of 5°C.min^{-1}. The morphology and size of the crystals were determined by scanning electron microscopy using a JEOL scanning electron microscope JSM-6610LV model. The Si/Al ratio of the crystals was determined by energy-dispersive X-ray (EDAX) analysis in the SEM chamber.

Nitrogen adsorption/desorption isotherms were determined by QUANTHACHROME 3B at 77 K. All samples were outgassed at 300°C under vacuum for 12 h. The specific surface area was determined by the BET equation.

Infrared transmission spectra (Ft-IR) of synthetic zeolites were obtained by the KBr wafer technique. The spectra were recorded on a FTIR-Spectrometer (Nicolet) in the region of 370-4000 cm^{-1} (middle range IR).

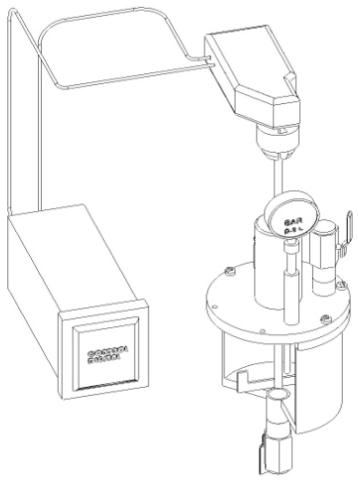

Figure 1: Equipment for synthesis of zeolites.

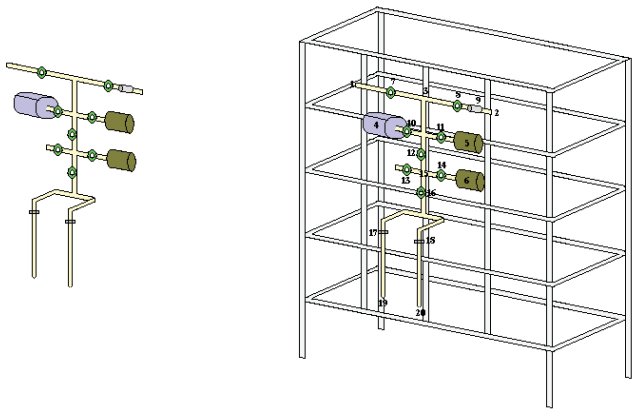

Figure 2: Adsorption Microcalorimeter: 1,2 Vacuum and gas injection. 3. Tube connecting. 4. Calibration volume. 5,6. Transducter pressure. 7-16. Valves presicion. 17,18 Cells calorimetrics.

TPD study

In order to study the acid and basic strength, ammonia was adsorbed on these zeolites. The NH_3 temperature programmed desorption (TPD) study was carried out using a heating rate of l0°C/min. Prior to TPD, 50 mg of the sample was placed in a pulse microreactor and calcined at 540°C. Then a series of 0.5 mL NH_3 pulses were given at 100°C. These pulses were continued until no more uptake of NH_3 was observed. Helium was then passed over the sample at a flow rate of 30 ml/min followed by the start of temperature programming. The desorbed NH_3 was detected by a thermal conductivity detector and the TPD profile was drawn.

Differential adsorption heats of zeolites

The heat of adsorption was measured in a heat flow microcalorimeter of the Tian-Calvet type (local construction, Figure 2) linked to a volumetric line that permitted the introduction of successive small pulses of ammonia gas. Before the calorimetric experiments a known amount of sample was heated in vacuo ($1 \bullet 10^{-3}$ Pa) for 6 h at 673 K.

Adsorption was carried out by introducing successive doses of a known amount of ammonia to the sample. For every adsorbed amount the equilibrium pressure was measured by means of a differential pressure gauge (Pfeiffer). Identical doses were sent repeatedly to the sample until a final equilibrium pressure of 0.5 Torr was obtained. The calorimetric and volumetric data were stored and analyzed by microcomputer processing. The adsorption temperature was maintained at 393 K to avoid physical adsorption.

Catalytic conversion of methanol

The zeolites synthesized were tested in the methanol conversion following the procedure described in [24]. The methanol conversion was carried out in a fixed bed reactor at 450°C under atmospheric pressure. Prior to each reaction, the samples (0.5g) were pretreated in he flow at 550°C for 2 h and cooled to the reaction temperature. Methanol (Sigma-Aldrich, C99.9%) was fed into the reactor by a liquid mass flow controller (Bronkhorst High-Tech, LIQUID-FLOW series L10/L20) and the weight hourly space velocity (WHSV) was 2.88 h^{-1}. A homogeneous mixture of MeOH (10%) and He (90%) was obtained

using a pre-heater to vaporize the methanol. All products were passed through a heated transfer line to a gas chromatograph with a thermal conductivity detector and a flame ionization detector (column: HP-PLOT Q, Agilent) in series.

Results and Discussion

Mordenite and HZMS-5

The diffractograms of materials prepared using the standard procedures for mordenite (HMOR) with seeds are presented in Figure 3a. The solid phase obtained was mordenite, according to comparison with a standard diffractogram [20-27]. The use of seeds for synthesis of HMOR produced materials with high crystallinity; the XRD powder pattern of the synthesized sample is shown in Figure 3b. Such a pattern is characteristic of ZSM-5 and is consistent with earlier work [23-30]. Specifically, the zone between 10 and 30 degrees has

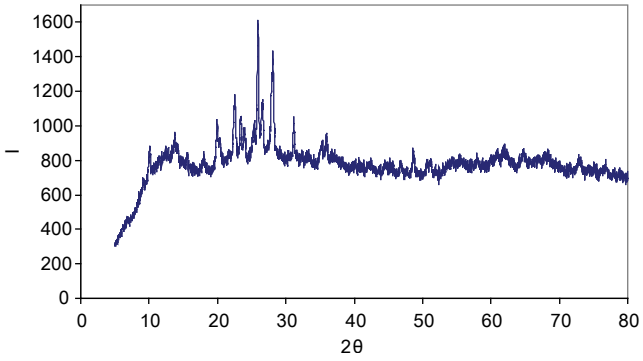

Figure 3a: XRD for Zeolite HMOR.

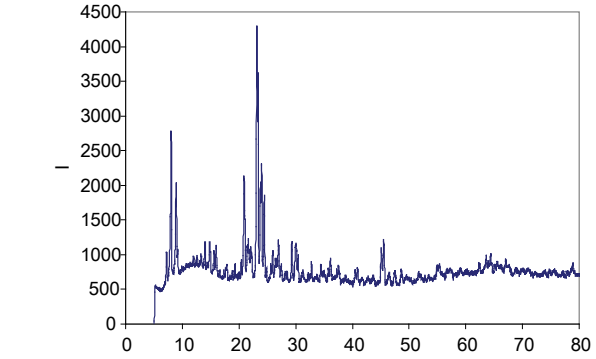

Figure 3b: XRD for Zeolite HZSM-5.

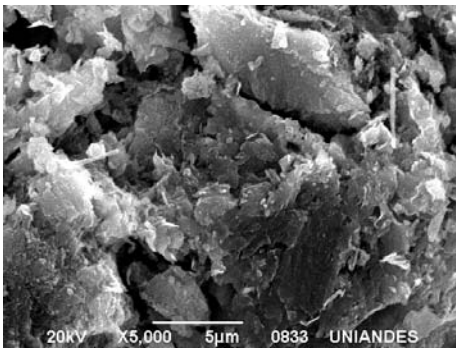

Figure 4: Scanning electron microscope of mordenite.

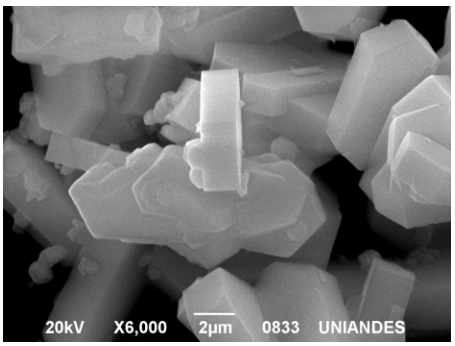

Figure 5: Scanning electron microscope of HZSM-5.

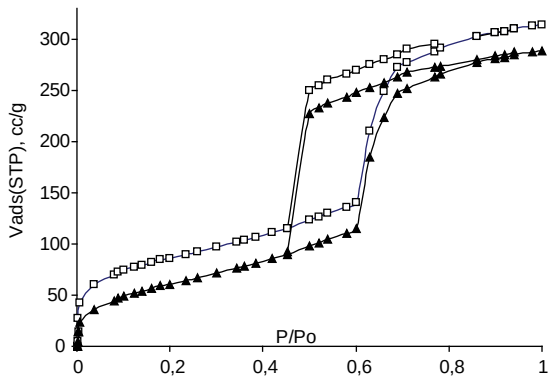

Figure 6: Adsorption isotherm of nitrogen at 77K on HMOR and HZSM-5.

the typical mordenite peaks, show that a zeolite ZSM5 has been obtained.

In the scanning electron micrograph of HMOR shown in Figure 4, crystals with two different morphologies can be seen: one being an acicular form, which is characteristic of mordenite, and another being a "ball of string" form that is a characteristic of these zeolites.

Figure 5 shows SEM micrographs of a highly crystalline material. The H-ZSM-5 sample displayed a hexagonal prismatic crystal morphology with different crystal sizes (three main crystal sizes of about 2µm x 5µm x 10µm were observed). No impurities were detected.

Physical adsorption

Nitrogen adsorption at 77 K on the standard samples is shown in Figure 6. The adsorption isotherms on HMOR and HZSM5 exhibited a well-defined hysteresis loop of type H1 according to the IUPAC classification [37]. This type of hysteresis loop was observed for the open ended cylindrical mesopores during adsorption and desorption.

The N_2 adsorption–desorption isotherms (cm^3/g sample) for the samples are shown in Figure 6. The larger adsorbed volume per gram sample is a result of the different type of zeolite synthesized. The micropore volume per gram sample increased from HMOR to HZSM5, as shown in Figure 6 and Table 1. Thus HMOR has a much higher mesopore volume compared to HZSM5. Up to the relative pressure at which hysteresis begins, the difference between the two isotherms in the volume adsorbed was less than 70cc/g. However, this difference abruptly increased as the mesopores were filled, giving differences as large as 120cc/g; the sample of HMOR had a higher pore volume than HZSM5.

		Microporosity		Mesoporosity		IR
Sample	S_{BET} ($m^2.g^{-1}$)	Volume ($cm^3.g^{-1}$)	size (nm)	Volume ($cm^3.g^{-1}$)	Sized (nm)	Crystalinity (%)
HZSM5	307	0.18	0.45	0.38	2-25	85.5
HMOR	389	0.21	0.50	0.41	2-35	90.0

Table 1: Textural characteristic of HMOR and HZSM-5and properties of infrared.

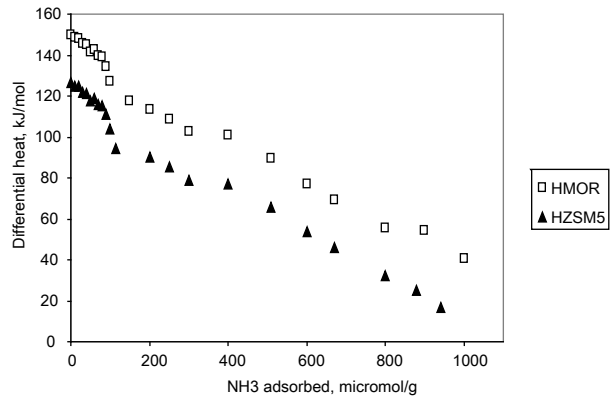

Figure 7: Differentials heats for HMOR and HZSM-5 were made 393 K.

The structural properties of the standard samples were obtained from both XRD and physical adsorption analysis and are shown in Table 1.

It can be seen that the HMOR sample had larger pore sizes, surface area, micropore volume and total pore volume than HZSM5. The wall thickness calculation based on the adsorption branch could not be obtained for HMOR since the pore diameter was higher than the a-parameter. The desorption branch finally closed for sample HMOR but the closure point was at low relative pressure when the normal point was around 0.45 relative pressure. This might be due to experimental error during the sorption isotherm measurement.

Adsorption heats of HZSM-5 and HMOR

Figure 7 shows the differential heats of adsorption of the samples at 393 K versus the adsorbed volume. It shows that there are a few acid sites that are able to strongly chemisorb ammonia at heats greater than 80kJ.mol^{-1} in HZSM5 compared to HMOR. Ammonia adsorption heats of above 80kJ.mol^{-1} may be either due to Bronsted or Lewis acid sites. The inflection point of the differential heat curves shows that the HZSM5 sample contained about 200µmol.g^{-1} of Lewis acid sites and the HMOR sample contained 390µmol.g^{-1}. The remaining sites were assigned to Bronsted acid sites.

FT-IR of HZSM-5 and HMOR

Similar two-band spectra have already appeared in the literature. It thus seems that the characteristic vibration of framework OH groups from Bronsted acid sites in H-ZSM-5 is around 3600 cm^{-1}. Since the latter band has been assigned to a well-defined vibration in the lattice, it follows that the environment for the framework hydroxyl groups in H-ZSM-5 is far less homogeneous. The existence of only a single framework OH vibration could mean that the groups are vibrating inside the small cages formed at the channel intersections. The absence of a band at 3720 cm^{-1} is indicative of highly crystalline material with negligible amounts of terminal silanols (due to the large crystal size) and without gel or other, not fully cross-linked, impurities.

HZSM5 shows a single OH band around 3600 cm^{-1}. Its rather large half-bandwidth indicates that the environment in which it was synthesized is less homogeneous given the very high degree of crystallinity of HZSM5 (as shown in SEM). This can be related to the A1 zoning reported for this zeolite [12, 22-34]. Presently, the catalytic consequences of the presence and/or absence of the 3720 cm^{-1} band in proton-catalyzed reactions are under investigation.

Figure 8 shows that the FT-IR spectra of synthesized HMOR are very similar to those of HZSM-5. In the FTIR of HZSM5 bands

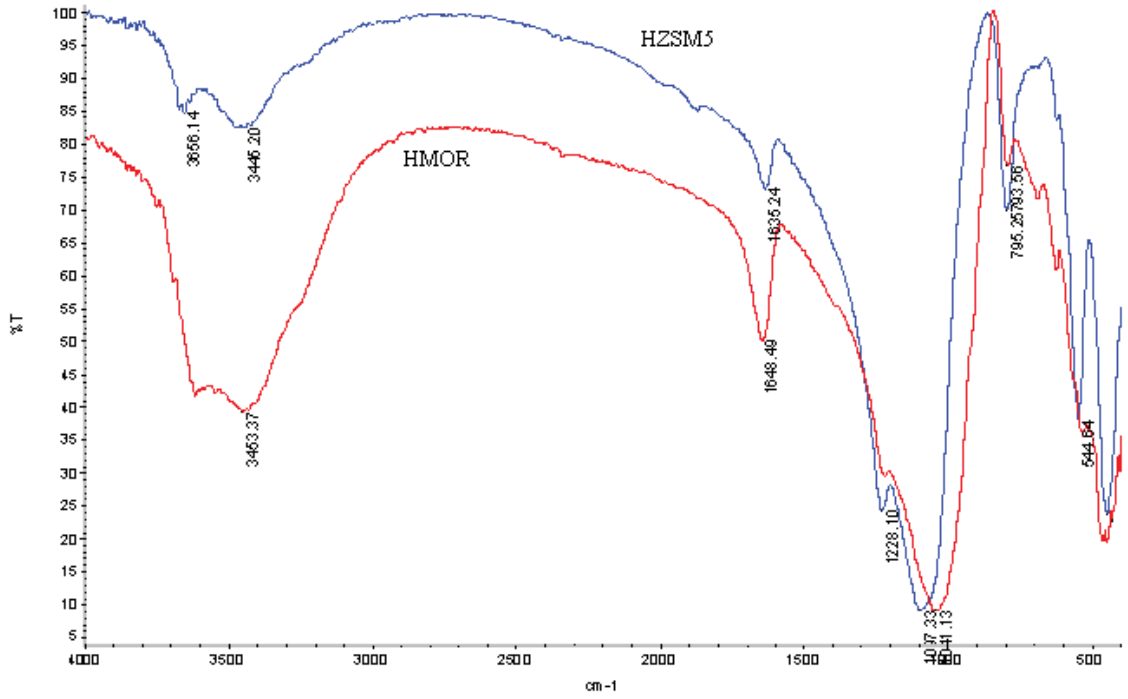

Figure 8: FTIR of HMOR and HZSM-5.

near 1080 cm^{-1} (internal asymmetric stretch), 790 cm^{-1} (external symmetric stretch), 542 cm^{-1} (double ring vibration) and 450 cm^{-1} (Si-O band) were apparent in all samples, due to the formation of the HZSM-5 phase. Additional evidence for the HZSM-5 zeolite was the asymmetric stretch vibration of the band at 1225 cm^{-1}, which has been assigned to external linkages (between the SiO_4 tetrahedral) and is a structure-sensitive IR band of HZSM-5 zeolite [20-24]. In the FT-IR spectra (Figure 8) an absorption signal corresponding to the MFI phase skeletal vibration is apparent at 542 cm^{-1}. Figure 8 shows the FT-IR spectra of HMOR obtained using kaolin. The spectra show the hydroxyls of HMOR after synthesis. There are two main peaks at 3749 and 3608 cm^{1}. According to previously reported results [20-32, 40-43] these two peaks should correspond to terminal silanols and framework Si–OH–Al groups, respectively. A small band at 3660 cm^{-1} is also apparent. This peak has previously been observed [24-27, 30-35, 43-45], and can be attributed to the hydroxyls associated with the ill-defined extra-framework alumina. The peaks in HMOR are more intense and defined.

The mordenite framework (Si/Al ratio=5) is characterized by the presence of straight channels running along the [001] crystallographic direction, which are accessible through twelve-membered (elliptical) silicon oxygen rings having dimensions of 0.65x0.70 nm (and hence slightly larger than those of ZSM-5, which are delimited by ten-membered rings with [0.51]0.55 nm radii). A second family of smaller channels intersects the previous one in the perpendicular [001] direction. These channels are delimited by eight-membered rings. Unlike ZSM-5, this second family of channels does not allow the full passage of molecules (even of small dimensions) from one straight channel to another. In fact the two halves of this second family of channels are slightly stacked, giving rise to narrow-necked obstructions. Summarizing, the mordenite structure shows only a set of permeable parallel straight channels with regularly disposed side pockets. The Si/Al ratio in mordenite (ca. 5) is lower than in ZSM-5 and, as a consequence, a larger number of counter cations, balancing the negative charge of the framework, are present. It is worth noticing that, with respect to H-ZSM-5 with the lowest Si/Al ratio (ca. 14); the proton density in H-Mord is larger by at least a factor of 3, which implies substantially lower distances between the Bronsted sites.

Temperature programmed desorption of ammonia (TPD) over HZSM-5 catalysts

Figure 9 shows the TPD profiles of HZSM-5 and HMOR with NH_3. For HZSM-5 with NH_3 adsorbed at 373 K the low temperature peak was observed at 453 K whereas the high temperature peak

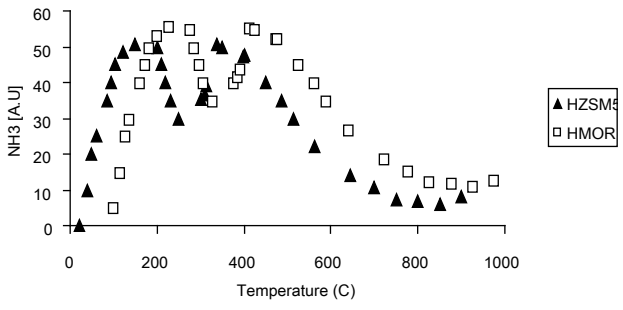

Figure 9: Temperature Programmed Desorption profiles of HMOR and HZSM5 and NH_3-TPD profiles of 373 K.

Catalyst	Conv.(%)	Selectivity (C-mol%)						P/E	Si/Al
		C_1-C_4[a]	C_2H_4	C_3H_6	C_4H_8	C5[b]	Aromatics		
HZSM5	92.6	18.5	18.0	22.7	8.25	12.6	20.0	1.75	42
HMOR	95.8	3.62	6.88	44.2	19.4	23.9	2.6	10.1	64

[a]C_1–C_4 saturated hydrocarbons
[b]C_5 and higher hydrocarbons excluding aromatics
[c]Reaction conditions: T=470 °C, WHSV = 1 h^{-1},P_{CH3OH}=0.5 atm,H_2O:CH_3OH = 1:1

Table 2: MTP reaction over unmodified and mesopore-modified HZSM-5 catalysts[c].

was observed at 653 K. The low temperature peak indicates weak acidic sites where ammonia molecules are weakly adsorbed. On the other hand the high temperature peak corresponds to strong acid sites present on the catalyst. The total amount of ammonia that was desorbed between 453 K and 553 K was 0.41 mmol of NH_3/g catalyst (HZSM-5). The HMOR catalysts with NH_3 adsorbed both at 523 K and 753 K predominantly show a peak with strong acidic sites only in the TPD profiles. Figure 9 depicts the TPD profile of HZSM-5 with varying amounts of acid sites per gram of catalyst (density of acid sites). HZSM-5 and HMOR catalysts have different TPD profiles; in the case of HMOR, which show some acid sites. The concentration of NH_3 desorbed up to 400 K was considered to indicate the amount of weak acid sites, and that coming out above 400 K was considered to indicate the amount of strong acid sites.

Role of acidic sites

In order to identify the type of sites that are responsible for MTP the following experiments were carried out. NH_3 was adsorbed on HZSM-5 catalyst samples at 373 K. These samples were used as the catalyst at 373 K. The TPD profiles of these catalysts are shown in Figure 8. In the case of HZSM-5 with NH_3 adsorbed at 453 and 653 K the conversion of MTP was only 8.5% with 89% selectivity to hydrocarbons in a 2-h run. Here all the strong acidic sites are blocked by NH_3 as NH_4^+ ions, whereas in the case of zeolite with NH_3 adsorbed at 653 K a fraction of strongly acidic sites are available. MTP takes place on these sites. The HMOR catalyst, which has more strong acidic sites (at 523 and 753 K), generates a high conversion percentage of MTP. This clearly proves that the weakly acidic sites have no activity while the strongly acidic sites are mainly responsible for MTP.

The methanol conversion and the selectivity (product distribution) of HZSM5 and HMOR are presented in Table 2. For the pure HZSM-5 (SiO_2/Al_2O_3 = 80), selectivity to C1–C4 saturated hydrocarbon, ethylene, propylene and butylene was 18.5, 18.0, 22.7 and 8.25 C mol%, respectively. Compared with HZSM-5, the propylene selectivity of the HMOR catalyst was double, while the C1–C4 saturated hydrocarbon selectivity increased and the butylene selectivity decreased. The changes in product distribution must be due to the major acidity of the HMOR catalyst: the propylene and butylene selectivity dramatically increased to 44.2 and 19.4C mol%, respectively, while the C1–C4 saturated hydrocarbon selectivity decreased to 3.62C mol% due to the decrease in strong acidity as well as the weakening of the strong acid strength.

The well-known methanol conversion consists of three main reaction steps. Methanol is dehydrated to dimethylether, and the resulting equilibrium mixture, consisting of methanol, dimethylether and water, undergoes further dehydration to produce light olefins. These are subsequently converted to paraffins, aromatics, naphthenes and higher olefins. These results are also associated with Si/Al ratios of zeolites; for over 100 relationships is contrary behavior.

The propylene selectivity is affected by the Brønsted acidity of the catalyst. In the case of HZSM-5 without Brønsted acidity,

methanol was not converted to hydrocarbon and the main product was dimethylether [16]. The changes in product selectivity with time on stream for HMOR are presented in Figure 10. The results are very similar to those reported in the literature [24] in terms of methanol conversion. However, in our case the higher percentage of conversion was obtained with HMOR. The trend is very similar to that reported by some authors, but our results show a higher variability is probably due to the sensitivity of our used method.

At the initial stage the selectivity to propylene and butylene increased slightly, whereas the selectivity to ethylene, saturated hydrocarbons and aromatics decreased slightly. After 25 h on stream the reaction reached the steady state. The methanol conversion over the HMOR catalyst after being on stream for 100 h is shown in Figure 10. However, the product selectivity's were similar to those at steady state. For the series catalysts, the propylene selectivity first increased

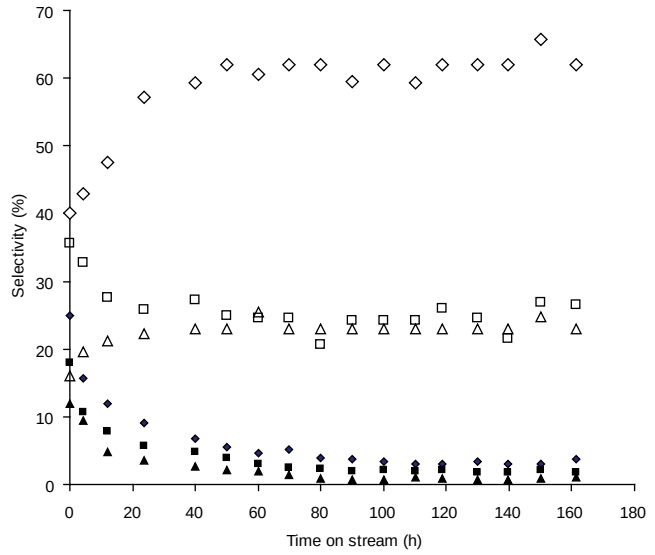

Figure 10: Product selectivity of HMOR as a representative catalyst for MTP reaction as a function of time: (◊) C_3H_6; (■) C_2H_4; (Δ) C_4H_8; (▲) aromatics; (♦) C_1–C_4 saturated hydrocarbons; (□) C_5 and higher hydrocarbons excluding aromatics. Reaction conditions: *T*=470 °C, WHSV=1h^{-1}, P_{CH3OH}=0.5 atm, H_2O:CH_3OH = 1:1.

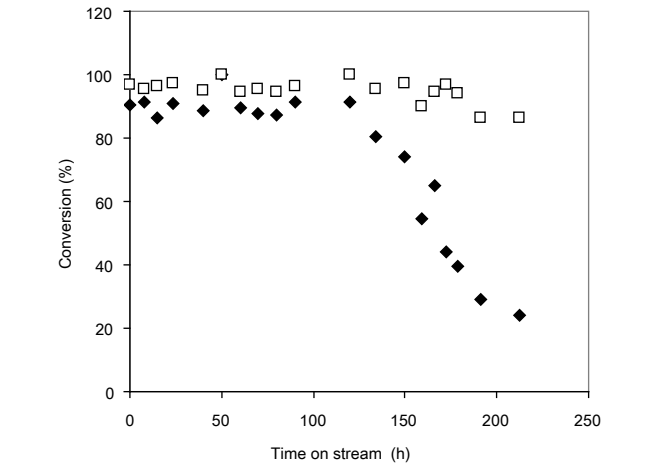

Figure 11: Catalytic stability of HMOR and HZSM-5 zeolites for MTP reaction: (□) HMOR; (♦) HZSM-5. Reaction conditions: T = 470°C, WHSV = 1 h^{-1}, P_{CH3OH} = 0.5 atm, H_2O:CH_3OH = 1:1.

and then decreased with an increase in the Si/Al ratio. The ethylene selectivity decreased gradually from 15.3 to 9.90%, as the Si/Al ratio increased. A decrease in the Brønsted acidity of the catalysts favored the formation of propylene in the reaction and led to an increase in the P/E ratio from 1.75 to 3.66. Meanwhile, the influence of mesopore modification on the product selectivity of the catalyst exceeded that of the acidity. For the HMOR catalyst, the propylene selectivity increased from 37.0 to 42.2% after modification, while the ethylene selectivity decreased from 10.1 to 4.18%, leading to a substantial increase in the P/E ratio from 3.66 to 10.1. It was noted that the selectivity to propylene and P/E ratio also improved on the HMOR catalyst. However, the improvement was less striking than that on the HZSM5 catalyst. The more probable reason is that the mesopores or cavities generated inside the zeolite crystals of HMOR catalyst by the method used, improved the diffusion of the gas molecules in the reaction process.

The catalytic stability of HMOR and HZSM-5 zeolites for the MTP reaction was tested at 470°C, and the results are shown in Figure 11. It can be seen that the catalytic stability followed the order of HMOR>HSZM5. As shown in Figure 11, the methanol conversion dropped abruptly after 10 minutes of stream. Coke deposition is the reason for catalyst deactivation [1]. When the coke accumulates to a certain level, it blocks the micropores of HZSM-5 and subsequently results in sharp deactivation of the catalyst. Additionally is should be observed that the catalytic stability that followed the order of HMOR > HSZM5, and that present a low propylene production and a low stability of HZSM-5 zeolite is due to that the Si/Al molar ratio of HZSM-5 used in this our work is low. In general, HZSM-5 zeolites with Si/Al ratio higher than 100. Additionally is should be observed that the catalytic stability that followed the order of HMOR > HSZM5, and that present a low propylene production and a low stability of HZSM-5 zeolite is due to that the Si/Al molar ratio of HZSM-5 used in this our work is low. In general, HZSM-5 zeolite with Si/Al ratio more than 100 exhibits good performance for MTP reaction exhibits good performance for MTP reaction.

Conclusions

In this work we synthesized HMOR and HZSM5 zeolites and were employed in the MTP process. The study of adsorption by means of nitrogen isotherms, scanning electronic microscopy and XRD demonstrated that the zeolites are synthesized by good percentage of crystalline.

HMOR converts methanol to propylene more effectively than HZSM-5 which associated with the ratio of Si/Al and with the different content of acid groups. This work shows novel results for this type of reaction and higher yields.

Acknowledgements

The authors would like to thank the Departments of Chemistry at the Universidad Nacional de Colombia and Universidad de Los Andes (Colombia) and the Master Agreement established between these two institutions. Special gratitude goes to the Fondo Especial de Investigaciones de la Facultad de Ciencias de la Universidad de Los Andes (Colombia) for its partial financing of this research.

References

1. Tanab K, Misono M, Ono Y, Hattori H, Delmon B, et al. (1989) New Solid Acids and Bases, Their Catalytic Properties, Studies in Surface Science and Catalysis. 51 Elsevier Amsterdam.
2. Huang Y, Havenga EA (2000) Probing the Locations of Benzene Molecules Inside Completely Siliceous ZSM-5 by FT-Raman Spectroscopy. J Phys Chem B 104: 5084-5089.
3. Hudee P, Novansky J, Silhar S, Trung TN, Zubec M, et al. (1986) Possibility of

using t-plots, obtained from nitrogen adsorption for the valuation of zeolites. Adsorpt Sci Technol 3: 159-164.

4. Rabo JA (1976) Zeolite Chemistry and Catalysis, ACS Monograph, 171, American Chemical Society, Washington, (Chapter 12).
5. Gregg SJ, Sing KSW (1982) Adsorption Surface Area and Porosity (2nd ed), Academic Press, London.
6. Jaroniec M, Madey R (1988) Physical Adsorption on Heterogeneous Solids, Studies in Physical and Theoretical Chemistry. 59 Elsevier, Amsterdam.
7. Saito A, Foley HC (1995) Argon porosimetry of selected molecular sieves: experiments and examination of the adapted Horvath-Kawazoe model. Micropo Mater 3: 531-542.
8. Saito A, Foley HC (1995) High-resolution nitrogen and argon adsorption on ZSM-5 zeolites: effects of cation exchange and Si Al ratio. Micropo Mater 3: 543-556.
9. Carolas-Amoros D, Alcaniz-Monge J, Linares-Solano A (1996) Characterization of activated carbon fibers by CO_2 adsorption. Langmuir 12: 2820-2824.
10. Brunauer S, Emmett PH, Teller E (1938) Adsorption of gases in multimolecular layers. J Am Chem Soc 60: 309-317.
11. Ghezini R, Sassi M, Bengueddach A (2008) Adsorption of carbon dioxide at high pressure over H-ZSM-5 type zeolite. Micropore volume determinations by using the Dubinin-Raduskevich equation and the *"t-plot"* Microporous Mesoporous Mater 113: 370-377.
12. Dubinin MM, Radushkevich LV, Zaveria ED (1947) Sorption and structure of active carbons. I. Adsorption of organic vapors. Zh Fiz Khim 21: 1351-1359.
13. Polanyi M, Verh MA, Deut (1914) Phys Ges. 16: 1012-1021.
14. De Boer JH, Linsen BG, Osinga TJ (1964) Studies on pore systems in catalysts. VI. The universal *t* curve J Catal 4: 643-649.
15. Payne DA, Sing KSW, Turk DH (1973) Comparison of argon and nitrogen adsorption isotherms on porous and nonporous hydroxylated silica. J Coll interf Sci 43: 287-293.
16. Brunauer S, Everett DH, Ottewill RH (1970) (Eds) Surface Area Determination, Butterworths.
17. Lecloux AJ, Pirard JP (1979) The importance of standard isotherms in the analysis of adsorption isotherms for determining the porous texture of solids. J Coll Inter Sci 70: 265-272.
18. Lecloux A J, Bronckart J, Noville F, Pirard JP (1988) The Generalized Broekhoff-De Boer Method. St Surf Sci Catal 39: 233-241.
19. Voogd P, Scholten JJF, Van Bekkum H (1991) Use of the *t*-plot—De Boer method in pore volume determinations of ZSM-5 type zeolites. Colloid Surf 55: 163-171.
20. Roque-Malherbe R (2000) Complementary approach to the volume filling theory of adsorption in zeolites. Microp Mesop Mater 41**:** 227-240.
21. Li B, Li S, Li N, Chen H, Zhang W, et al. (2006) Structure and acidity of Mo/ZSM-5 synthesized by solid state reaction for methane dehydrogenation and aromatization. Microporous Mesoporous Mater 88: 244-253.
22. Lee KY, Lee HK, Ihm SK (2010) Influence of Catalyst Binders on the Acidity and Catalytic Performance of HZSM-5 Zeolites for Methanol-to-Propylene (MTP) Process: Single and Binary Binder System. Top Catal 53: 247-253.
23. Lee YJ, Kim YW, Viswanadham N, Jun KW, Bae JW (2010) Novel aluminophosphate (AlPO) bound ZSM-5 extrudates with improved catalytic properties for methanol to propylene (MTP) reaction. Appl Catal A 374: 18-25.
24. Me C, Wen P, Liu Z, Liu H, Wang Y, et al. (2008) Selective production of propylene from methanol: Mesoporosity development in high silica HZSM-5. J Catal 258: 243–249.
25. Firozzi M, Baghalha M, Asadi M (2009) The effect of micro and nano particle sizes of H-ZSM-5 on the selectivity of MTP reaction. Catal Commun 10**:** 1582-1585.
26. Lin J, Zhang C, Shen Z, Hua W, Tang Y, et al. (2009) Methanol to propylene: Effect of phosphorus on a high silica HZSM-5 catalyst. Catal Commun 10: 1506-1509.
27. Gregg SJ, Rouquerol J, Sing KSW (1982) Adsorption at the Gas–Solid and Liquid–Solid Interface Elsevier.
28. Lee YJ, Kim YW, Jun KW, Viswanadham N, Bae JW (2009) Textural properties and catalytic applications of ZSM-5 monolith foam for methanol conversion. Catal Lett 129: 408-415.
29. Raznjevic K (1970) Tables et diagrammes thermodinamiques editions, Eyrolles 558-591.
30. Remy MJ, Poncelet G (1995) A new approach to the determination of the external surface and micropore volume of zeolites from the nitrogen adsorption isotherm at 77 K. J Phys Chem 99: 773-779.
31. Muller U, Unger KK (1988) Sorption Studies on Large ZSM-5 Crystals: The Influence of Aluminium Content, The Type of Exchangeable Cations and the Temperature on Nitrogen Hysteresis Effects. Stud Surf Sci Catal 39: 101-108.
32. Pieterse JAZ, Booneveld S, Van den Brink RW (2004) Evaluation of Fe-zeolite catalysts prepared by different methods for the decomposition of N_2O. Appl Catal B 51: 215-228.
33. Golden TC, Sircar S (1994) Gas Adsorption on Silicalite. J Colloid Interface Sci 162: 182-188.
34. IUPAC (1985) Pure Appl Chem 57: 603-611.
35. Bering BI, Dubinin MM, Sepinskii UU (1972) On thermodynamics of adsorption in micropores. J Colloid Interface Sci 38: 185-194.
36. Dubinin MM (1975) Adsorbtsiya I Poristos: Izdatels vo, BAXZ, Moskva, 1972. Prog Surf Membr Sci 9: 1-10.
37. Dubinin MM (1977) Am Chem Soc Sym Ser 40: 1-12.
38. Datka J, Piwowarska Z, Rakoczy J, Sulikowski B (1988) Catalytic and acid properties of pentasil zeolites: Isomerization of *o*-xylene and alkylation of toluene. Zeolites 8: 199-204.
39. Nayak VS, Choudhary VR (1983) Acid strength distribution and catalytic properties of H-ZSM-5: Effect of deammoniation conditions of NH4-ZSM-5. J Catal 81: 26-32.
40. Babu GP, Hegde DG, Kulkarmi SB, Ratnasamy P (1983) Active centres over HZSM5 zeolites : I. Xylene isomerization. J Catal 81: 471-477.
41. Narayanan S, Sultana A, Krishna K (1994) Aniline alkylation over MFI zeolites and its relation to stepwise desorption of ammonia. Reat Kinet Catal Lett 52: 205-210.
42. Bhandarkar V, Bathia S (1994) Selective formation of ethyltoluene by alkylation of toluene with ethanol over modified HZSM-5 zeolites. Zeolites 14: 439-449.
43. Narayanan S, Kumari VD, Rao AS (1994) Vapour phase aniline alkylation activity and selectivity over H-ZSM-5. Appl Catal A Gen 111: 133-142.
44. Vedrine JC, Auroux A, Bolis V, Dejaifve P, Naccache C, et al. (1979) Infrared, microcalorimetric, and electron spin resonance investigations of the acidic properties of the H-ZSM-5 zeolite. J Catal 59: 248-262.
45. Topsoe NY, Pedersen K, Derouane EG (1981**)** Infrared and temperature-programmed desorption study of the acidic properties of ZSM-5-type zeolites. J Catal 70: 41-52.
46. Kapustin GI, Brueva TR, Klyachko AL, Beran S Wichterlova B (1988) Determination of the number and acid strength of acid sites in zeolites by ammonia adsorption. Comparison of calorimetry and temperature-programmed desorption of ammonia. Appl Catal 42: 239-249.
47. Auroux A, Bolis V, Wierzchowski P, Gravelle PG, Vedrine JC (1979) Study of the acidity of ZSM-5 zeolite by microcalorimetry and infrared spectroscopy. J Chem Soc Faraday Trans I 15: 2544-2555.
48. Choudhary VR, Pataskar SG (1986) Step-wise thermal desorption of ammonia from X, Y and ZSM-5 type zeolites. Zeolites 6: 307-311.
49. Narayanan S, Deshpande K (1996) A comparative aniline alkylation activity of montmorillonite and vanadia-montmorillonite with silica and vanadia-silica. Appl Catal A 135: 125-135.
50. Narayanan S, Sultana A, Krishna K, Meriaudeau P, Naccache C (1995) Synthesis of ZSM-5 type zeolites with and without template and evaluation of physicochemical properties and aniline alkylation activity. Catal Lett 34: 129-138.
51. Wallau M, Schuth F, Brenner A, Melson S, Spichtuger P, et al. (1992) in R. Von Ballmoos, J.B. Higgins and M.M.J. Treacy (Eds). Proceedings of (5th International Zeolite Conference), Montreal, Butterworth-Heinemann.
52. Narayanan S, Deshpande K (1995) Mechanism of aniline alkylation over vanadia and supported vanadia. J Mol Catal 104: 109-113.

53. Song W, Justice RE, Jones CA, Grassian VH, Larsen SC (2004) Synthesis, characterization, and adsorption properties of nanocrystalline ZSM-5. Langmuir 20: 8301-8306.

54. Kim SS, Shah J, Pinnavaia TJ (2003) Colloid-imprinted carbons as templates for the nanocasting synthesis of mesoporous ZSM-5 zeolite. Chem Mater 15: 1664-1668.

55. Yamamura M, Chaki K, Wakatsuki T, Okado H, Fujimoto Z (1994) Synthesis of ZSM-5 zeolite with small crystal size and its catalytic performance for ethylene oligomerization. Zeolites 14: 643-649.

56. Mintova S, Bein T (2001) Microporous films prepared by spin-coating stable colloidal suspensions of zeolites. Adv Mater 13: 1880-1883.

57. Reding G, Maureer T, Kraushaar-Czarnetzki B (2003) Comparing synthesis routes to nano-crystalline zeolite ZSM-5. Micropor Mesopor Mater 57: 83-94.

58. Schoeman BJ, Sterte J, Ottstedt JE (1993) Synthesis and size tailoring of colloidal zeolite particles. Chem Commun 12: 994-1002.

59. Van Grieken R, Sotelo JL, Menendez JM, Melero JA (2000) Anomalous crystallization mechanism in the synthesis of nanocrystalline ZSM-5. Micropor Mesopor Mater 39: 135-147.

60. Kentgens APM, Iuga D, Kalwei M, Koller H (2001) Direct observation of brønsted acidic sites in dehydrated zeolite H-ZSM5 using DFS-enhanced 27Al MQMAS NMR spectroscopy. J Am Chem Soc 123: 2925-2926.

61. Boronat M, Viruela PM, Corma A (2004) Reaction intermediates in acid catalysis by zeolites: prediction of the relative tendency to form alkoxides or carbocations as a function of hydrocarbon nature and active site structure. J Am Chem Soc 126: 3300-3313.

62. Van Bokhoven JA,Van der Eerden AMJ, Prins R (2004) Local structure of the zeolitic catalytically active site during reaction. J Am Chem Soc 126: 4506-4507.

63. Zhang W, Ma D, Liu X, Bao X (1999) Perfluorotributylamine as a probe molecule for distinguishing internal and external acidic sites in zeolites by high-resolution 1H MAS NMR spectroscopy. Chem Commun 5: 1091-1102.

64. Zheng S, Heydenrych HR, Jentys A, Lercher JA (2002) Influence of surface modification on the acid site distribution of HZSM-5. J Phys Chem B 106: 9552-9558.

65. Takahara I, Saito M, Matsuhashi H, Inaba M, Murata K (2007) Increase in the number of acid sites of a H-ZSM5 zeolite during the dehydration of ethanol. Catalysis Letters 113: 3-4.

66. KY Wang, XS Wang, G Li (2007) A study on acid sites related to activity of nanoscale ZSM-5 in toluene disproportionation. Catal Commun 8: 324-332.

67. Wang KY, Wang XS, Li G (2006) Quantitatively study acid strength distribution on nanoscale ZSM-5. Micropor Mesopor Mater 94: 325-329.

68. Hudek P, Bobok D, Smiesková A, Zídek Z (1996) Sorption and diffusion properties of H- and modified forms of ZSM-5 zeolites. Adsorpt Sci Techonol 13: 495-508.

69. Bhattacharya D, Sivasanker S (1995) A comparison of aromatization activities of the medium pore zeolites, zsm-5, zsm-22, and eu-1. J Catal 153: 353-355.

70. Zhang W, Han X, Liu X, Lei H, Liu X, et al. (2001) Xenon probe for detecting the microporous structure of nanosized HZSM-5 zeolite. Chem Commun 1: 293-294.

71. Zhang W, Han X, Liu X, Lei H, Liu X, et al. (2002) Investigation of the microporous structure and non-framework aluminum distribution in dealuminated nanosized HZSM-5 zeolite by ^{129}Xe NMR spectroscopy. Micropor Mesopor Mater 53: 145-157.

72. Rudzinski W, Narkiewicz-Michalek J, Szabelski P (1997) Adsorption of aromatics in zeolites ZSM-5: A thermodynamic-calorimetric study based on the model of adsorption on heterogeneous adsorption sites. Langmuir 13: 1095-1103.